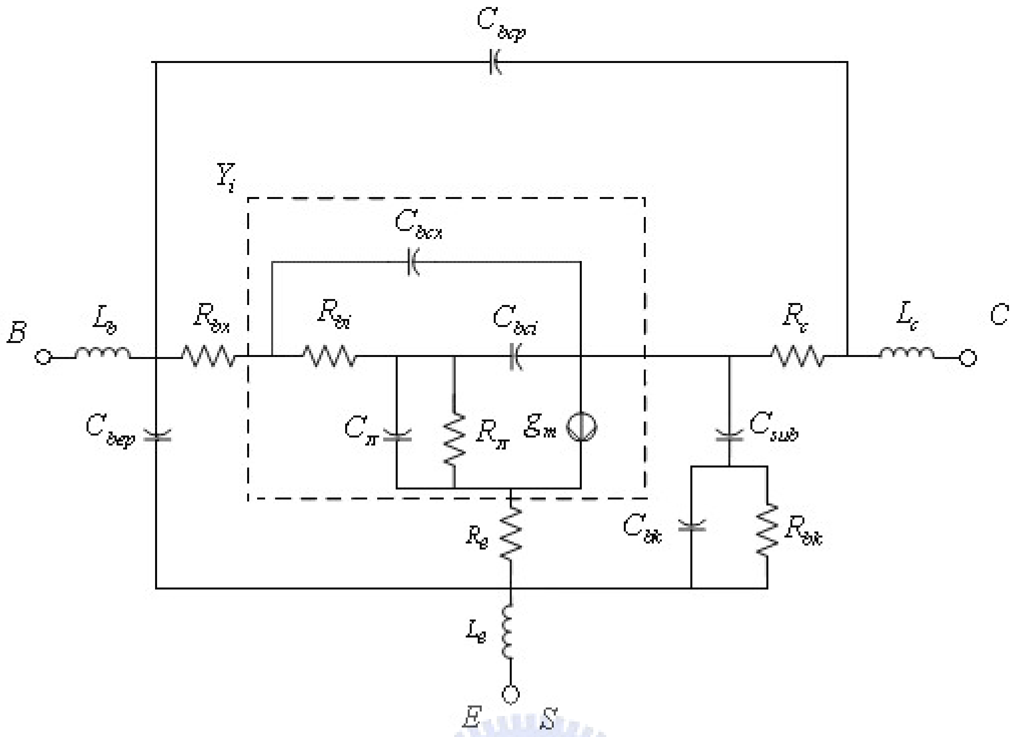

Fig.2-1 Small-signal equivalent circuit model for a SiGe HBT in the forward active region.

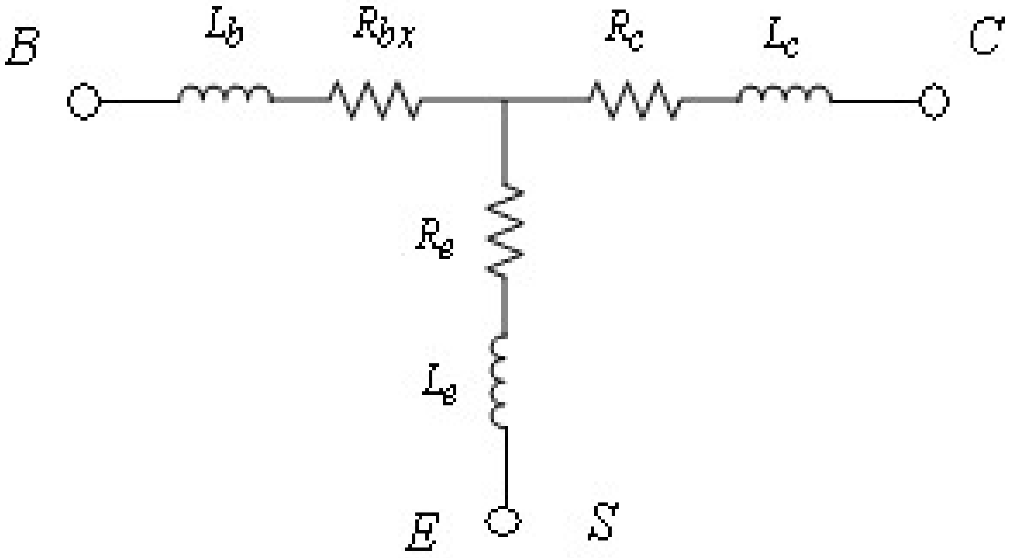

Fig.2-2 Equivalent circuit for a SiGe HBT at open-collector bias condition.

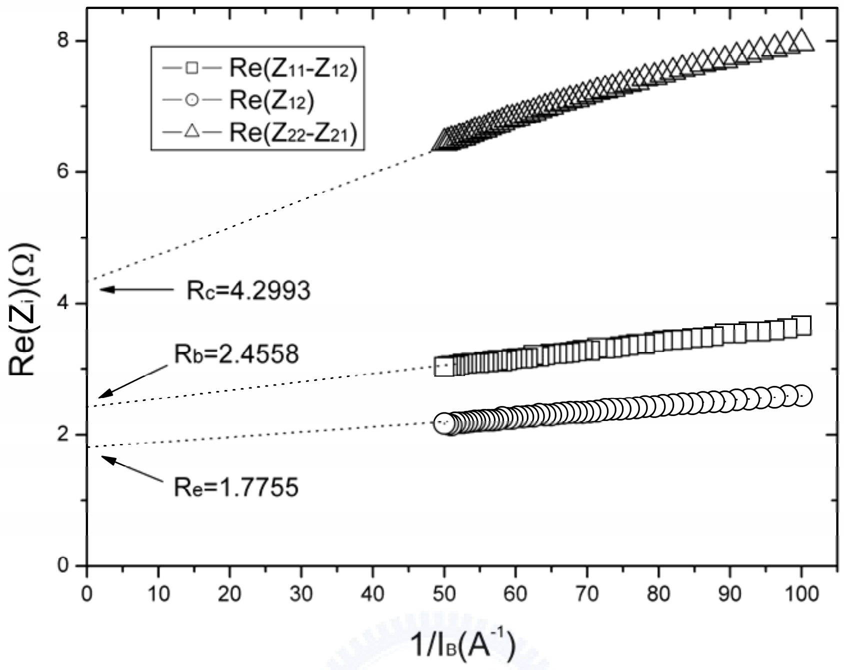

(a)

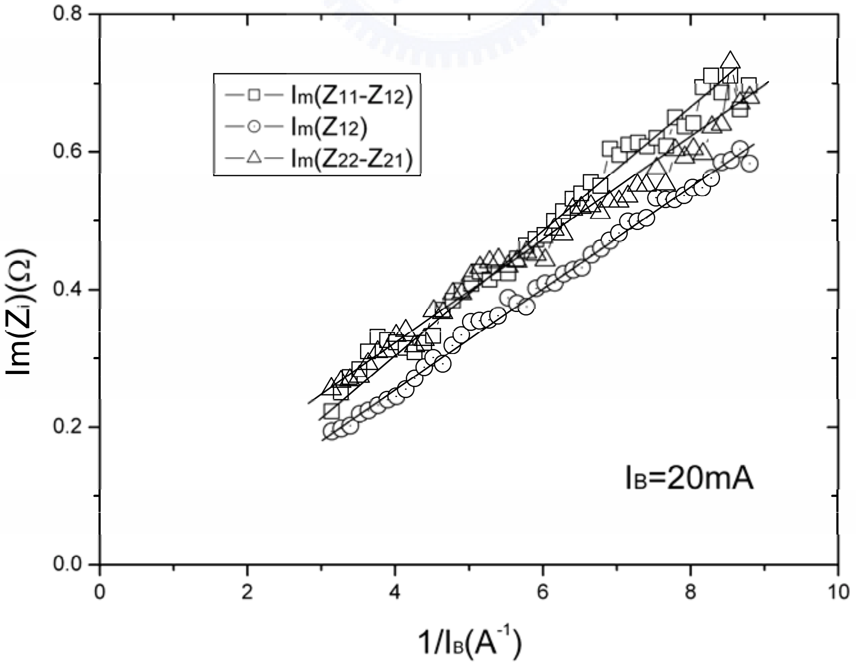

(b)

Fig.2-3 (a) Plot of Re(Z_{22}–Z_{21}), Re(Z_{11}–Z_{12}), and Re(Z_{12}) versus 1/I_B, freq = 1.0GHz. (b) Evolution of the Im(Z_{11}–Z_{12}), Im(Z_{12}), and Im(Z_{22}–Z_{21}) versus ω when the device is biased at high base current density (I_B=40 mA).

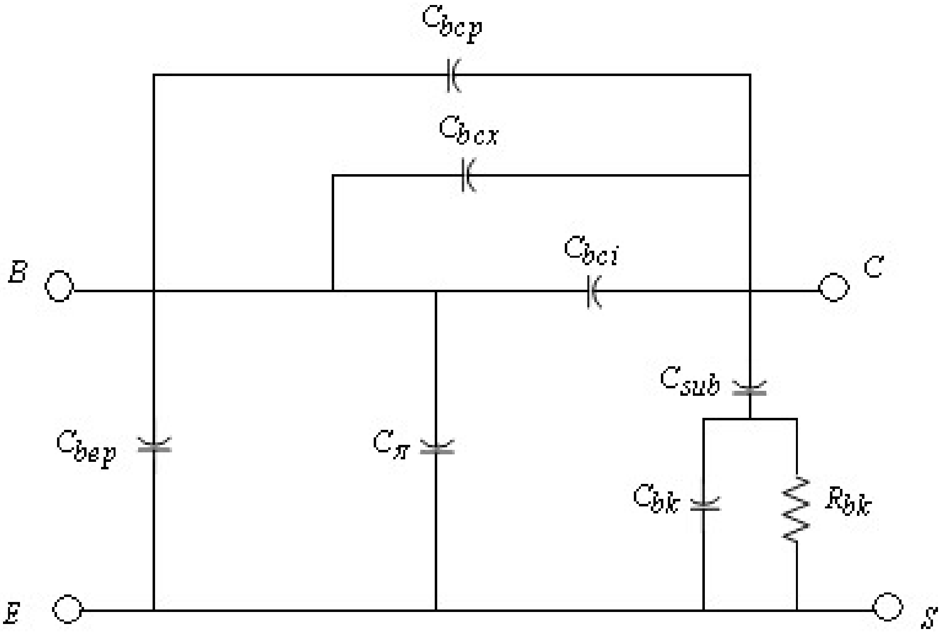

Fig.2-4 Small-signal equivalent circuit model for a SiGe HBT biased at V_{CE}=0 and reverse and/or low forward base voltage after de-embedding the "open" dummy pad.

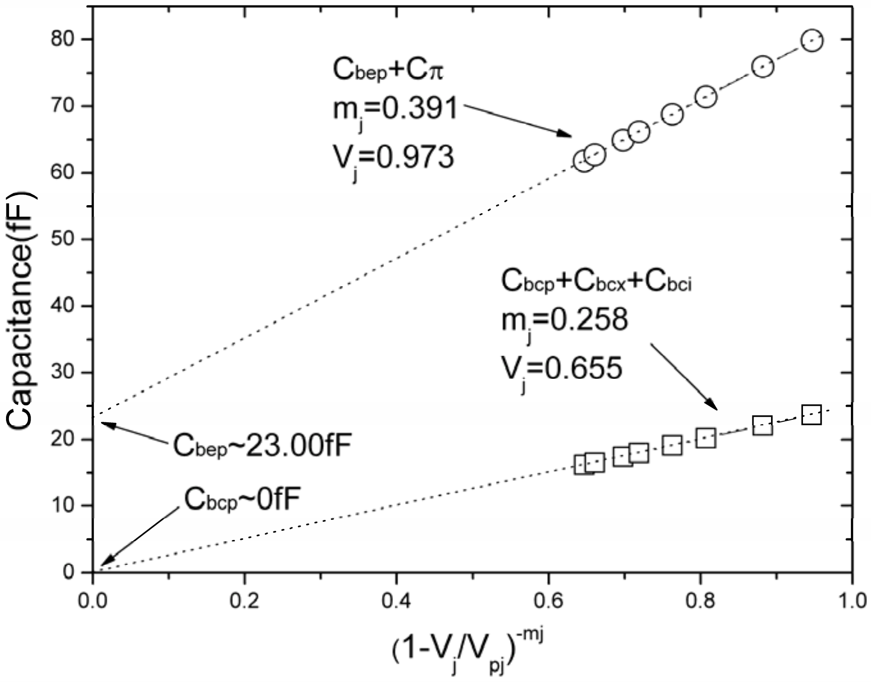

Fig. 2-5 Measured capacitances ($C_{bep}+C_\pi$) and ($C_{bcp}+C_{bcx}+C_{bci}$) versus the expression of $(1-V_j/V_{Pj})^{-mj}$.

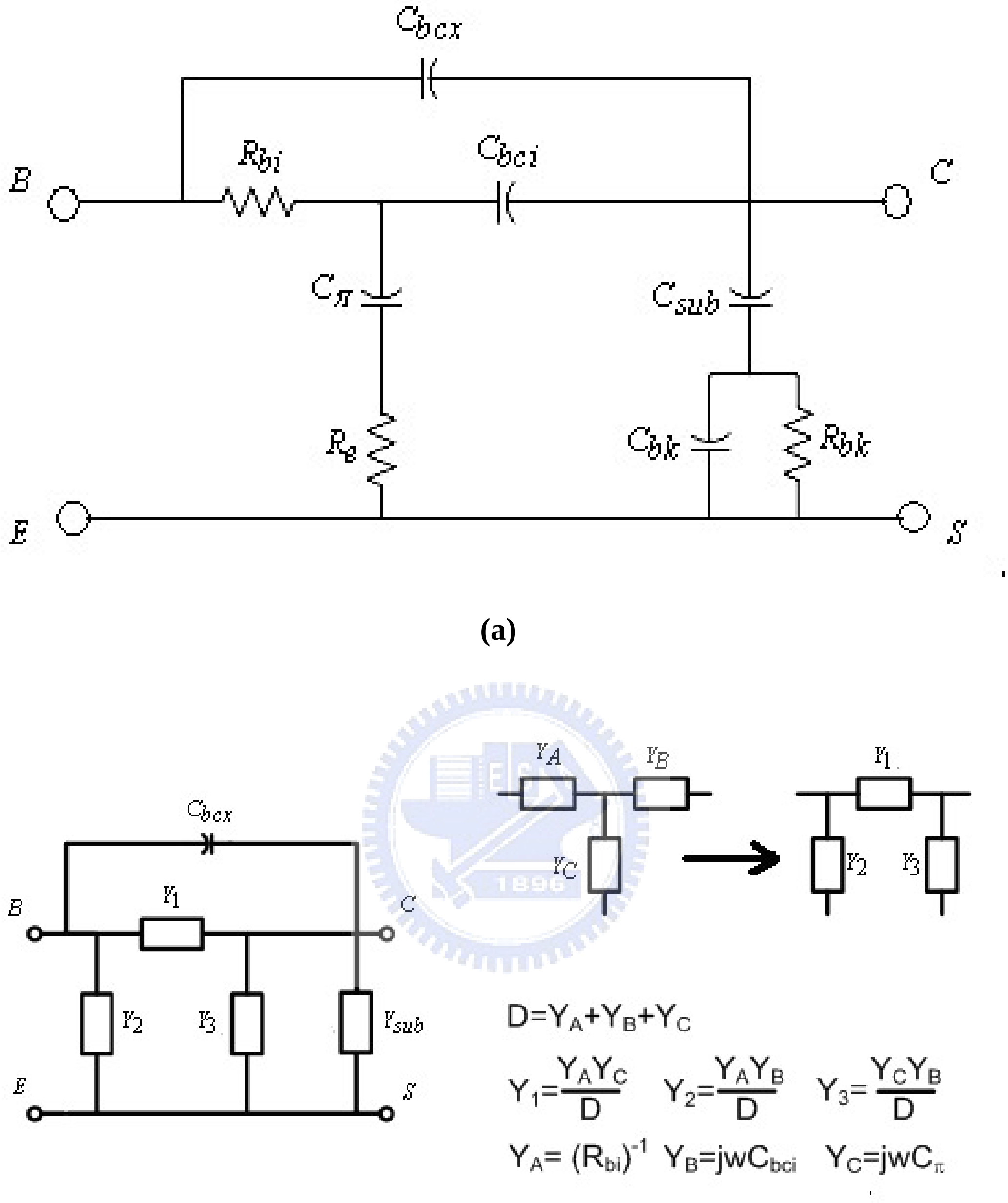

$$D=Y_A+Y_B+Y_C$$

$$Y_1=\frac{Y_AY_C}{D} \quad Y_2=\frac{Y_AY_B}{D} \quad Y_3=\frac{Y_CY_B}{D}$$

$$Y_A=(R_{bi})^{-1} \quad Y_B=jwC_{bci} \quad Y_C=jwC_\pi$$

(a)

(b)

Fig.2-6 (a) Small-signal equivalent circuit model for a SiGe HBT biased at V_{BE}=0 and forward and/or low reverse collector voltage after de-embedding the "open" dummy pad and removing the extrinsic inductances, extrinsic base resistance and extrinsic collector resistance. (b) Application of the T↔Π transformation to the HBT device equivalent circuit shown in (a).

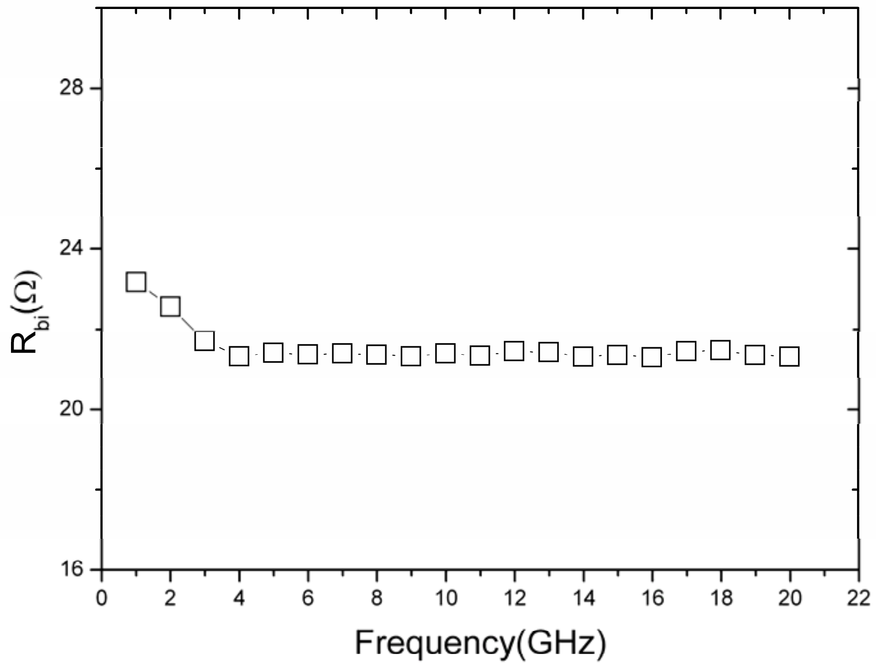

Fig.2-7 Frequency dependencies of the extracted R_{bi} for a SiGe HBT biased at V_{BE}=0V and V_{CE}=3V.

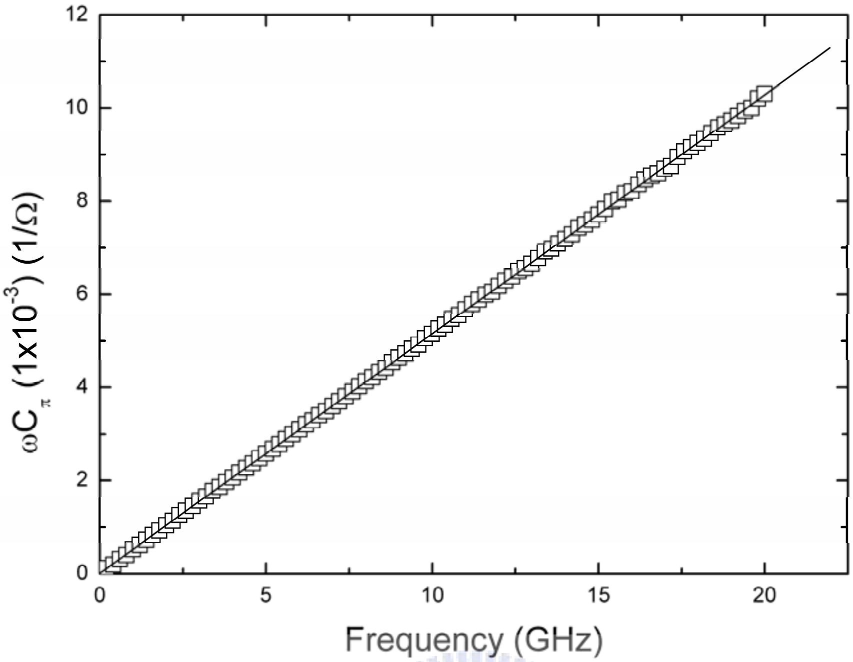

Fig.2-8 Frequency dependencies of the extracted ωC_{π} for a SiGe HBT biased at V_{BE}=0V and V_{CE}=3V.

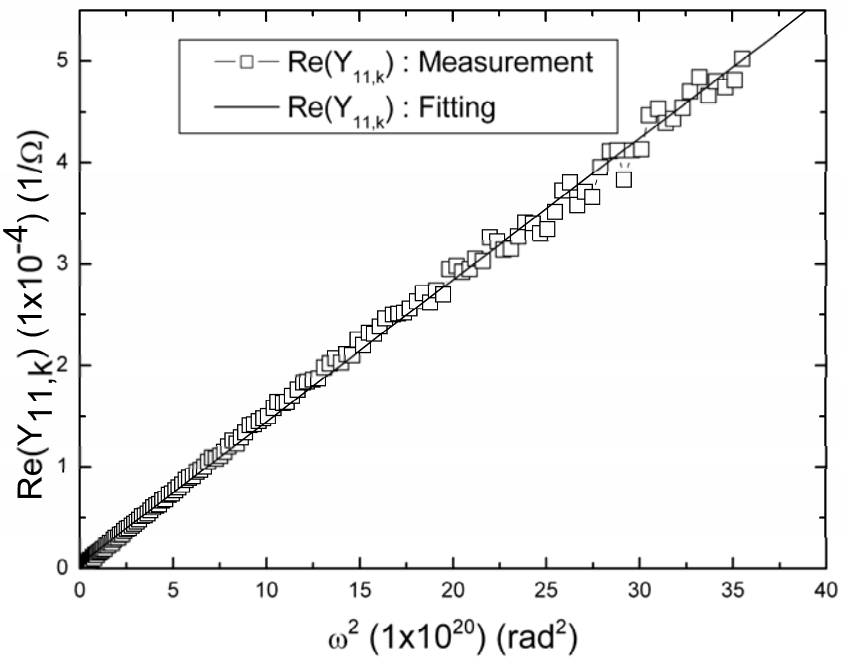

Fig.2-9 Plot of Re($Y_{11,k}$) versus ω^2 for the calculation of C_{bci} for a SiGe HBT biased at V_{BE}=0V and V_{CE}=3V.

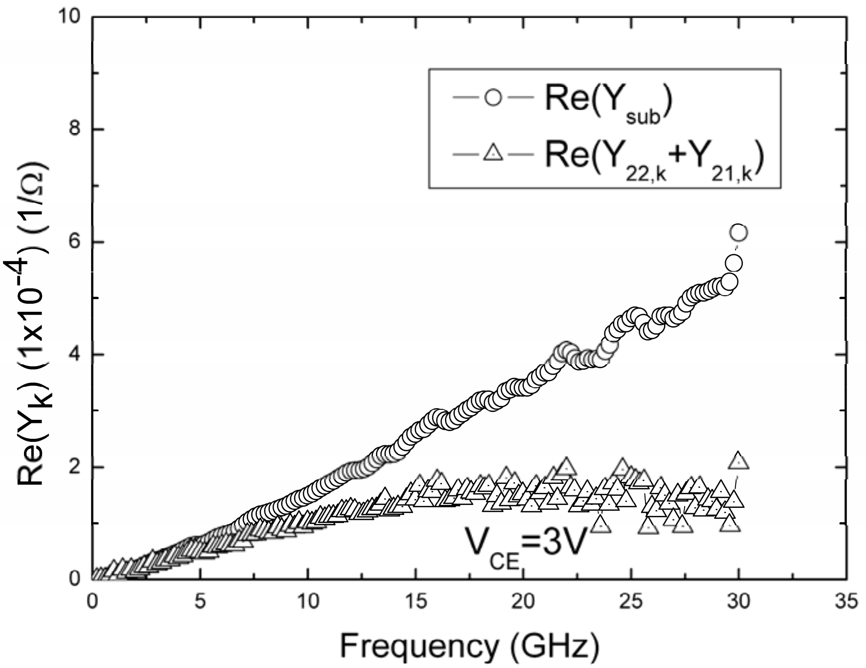

Fig.2-10 Plot of frequency dependence of the extracted $\mathrm{Re}(Y_{sub})$ and $\mathrm{Re}(Y_{22,k}+Y_{21,k})$ biased at V_{BE}=0V and V_{CE}=3V.

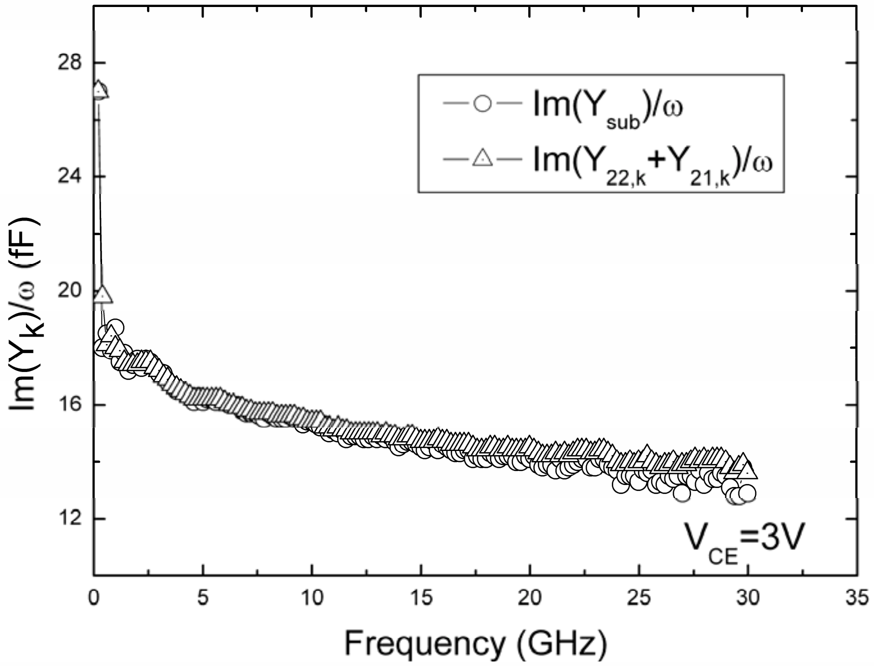

Fig.2-11 Plot of frequency dependence of the extracted Im(Y_{sub}) and Im($Y_{22,k}$+$Y_{21,k}$) biased at V_{BE}=0V and V_{CE}=3V.

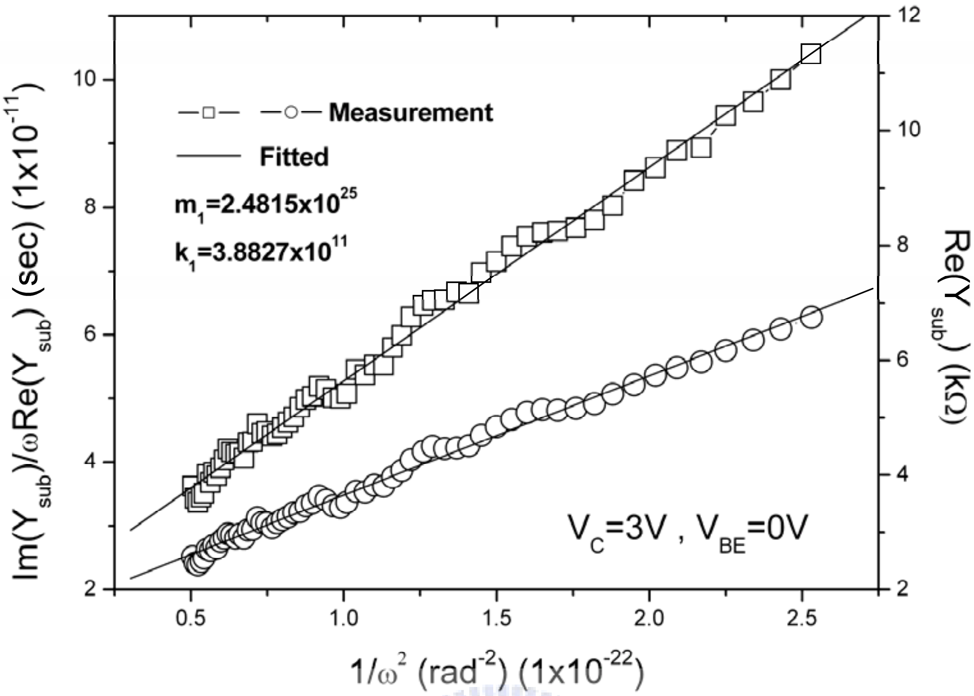

Fig.2-12 Plot of Im(Y_{sub})/(ωRe(Y_{sub})) and Re(Y_{sub}) versus 1/ω for a SiGe HBT biased at V_{BE}=0V and V_{CE}=3V.

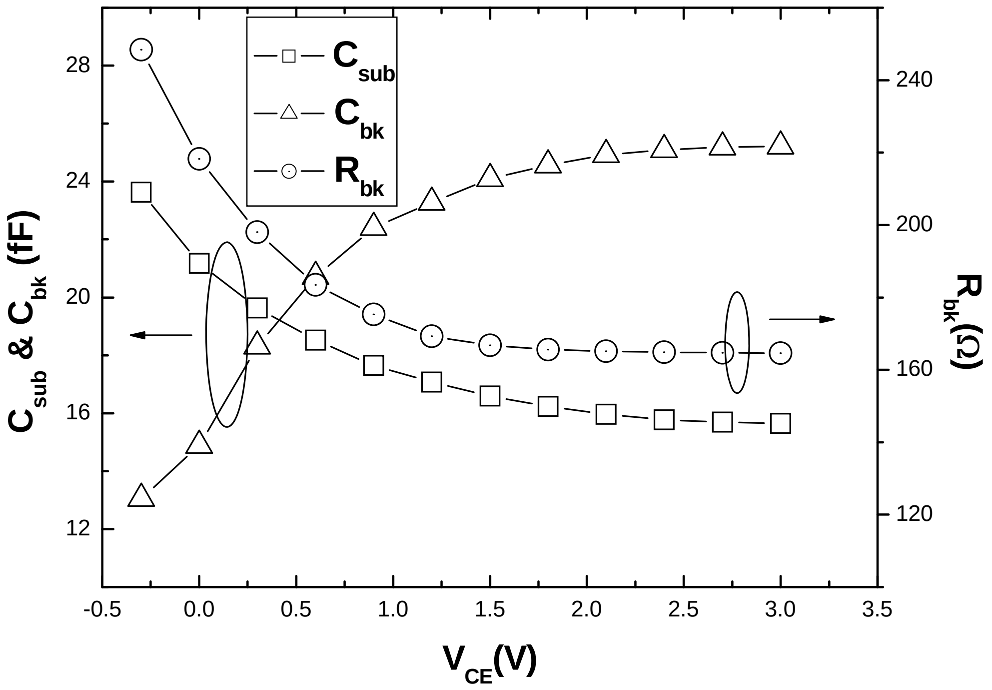

Fig.2-13 Collector-voltage dependence of the extracted C_{sub}, R_{bk} and C_{bk} for a SiGe HBT biased at V_{BE}=0V and V_{CE}=3V.

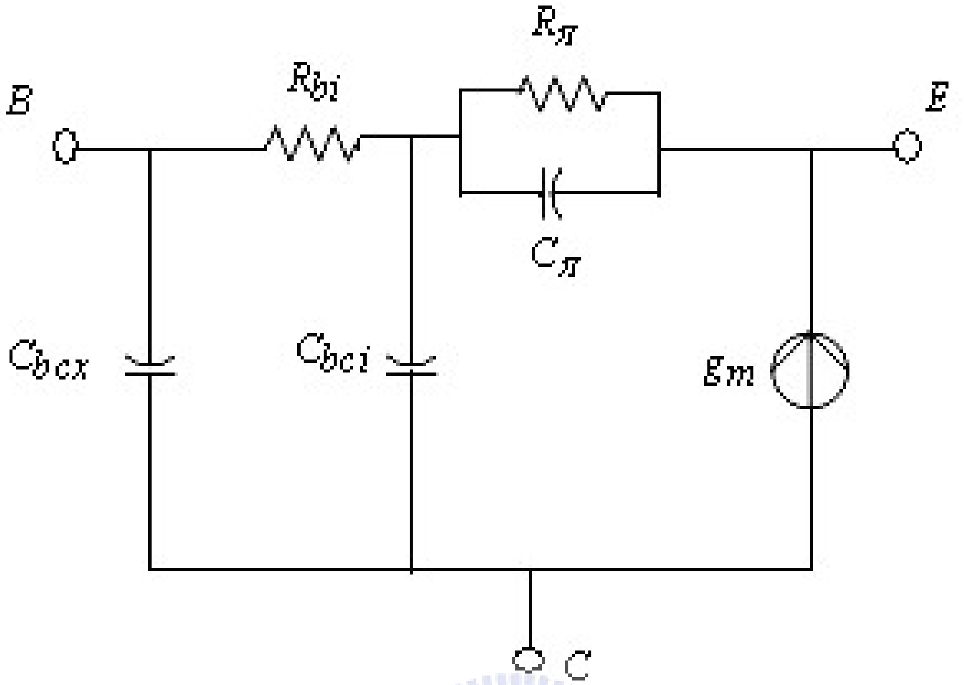

Fig.2-14 Small-signal equivalent circuit model of intrinsic SiGe HBT in common collector configuration.

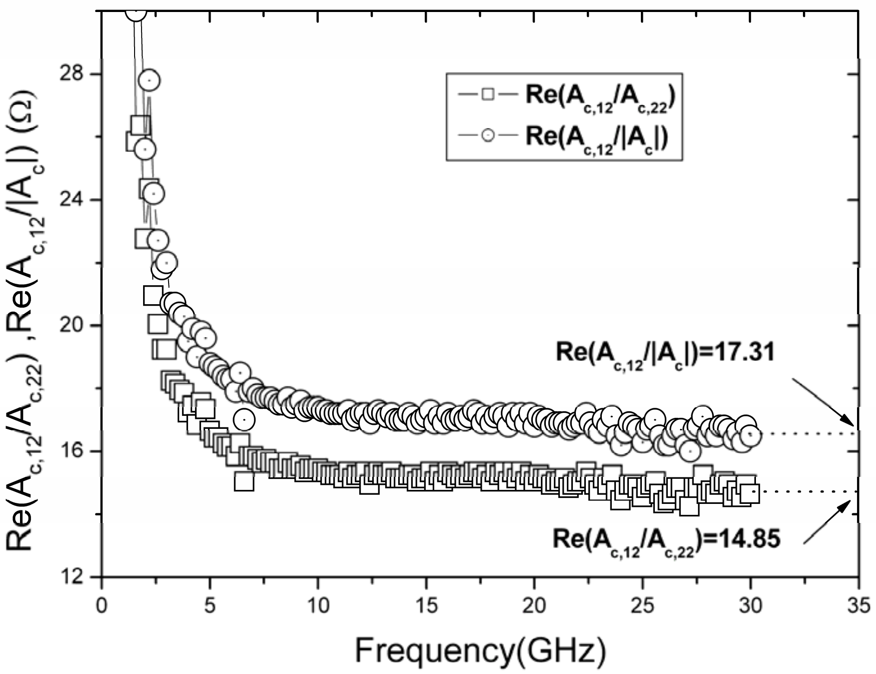

Fig.2-15 Plot of Re($A_{c,12}/A_{c,22}$) and Re($A_{c,12}/|A_c|$) versus frequency. V_{BE}=0.83V, V_{CE}=3V, I_C=1.516mA, and I_B=9.136μA.

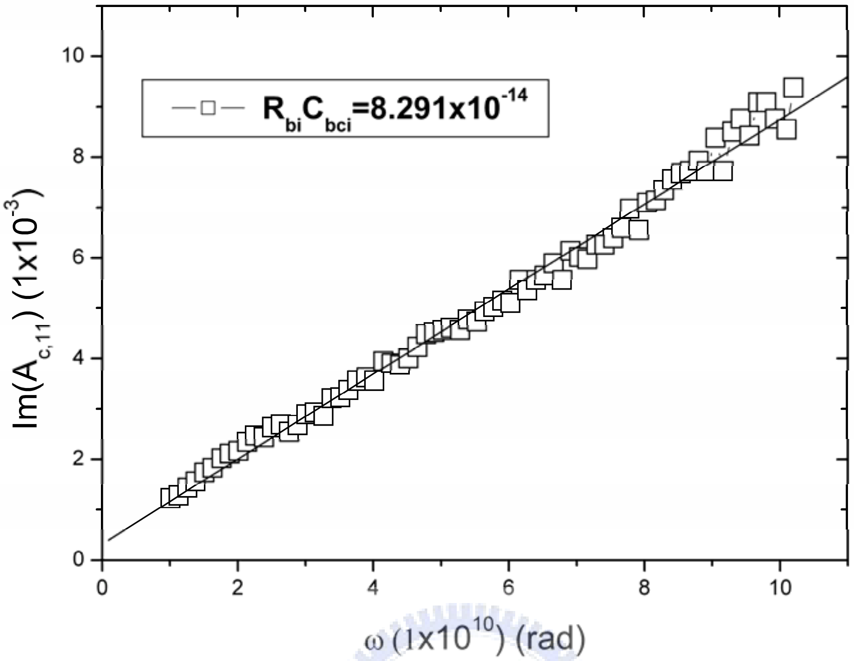

Fig.2-16 Plot of Im($A_{c,11}$) versus ω. V_{BE}=0.83V, V_{CE}=3V, I_C=1.516mA, and I_B=9.136μA.

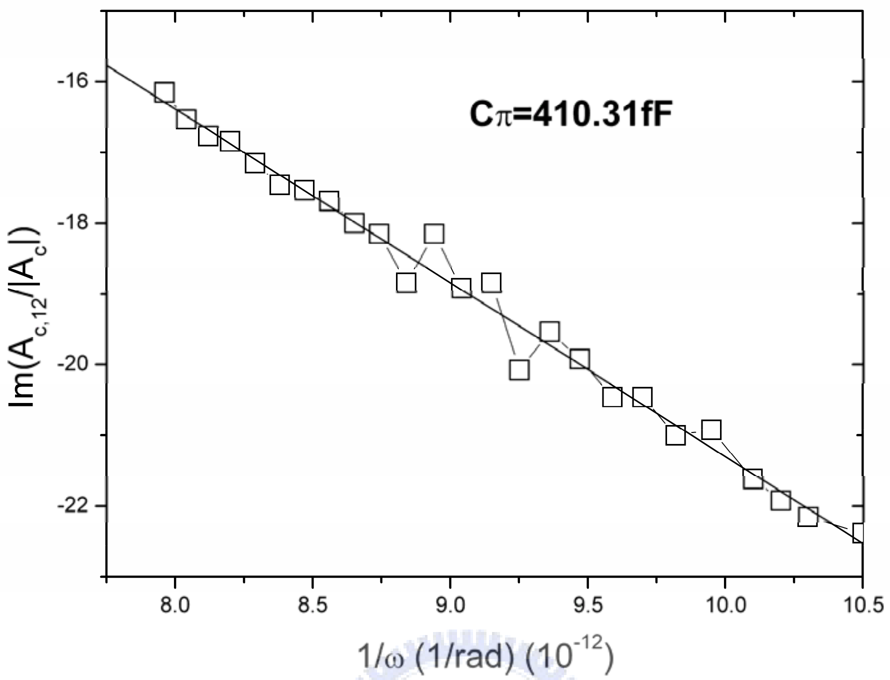

Fig.2-17 Plot of Im($A_{c,12}$/|A_c|) versus 1/ω. V_{BE}=0.83V, V_{CE}=3V, I_C=1.516mA, and I_B=9.136μA.

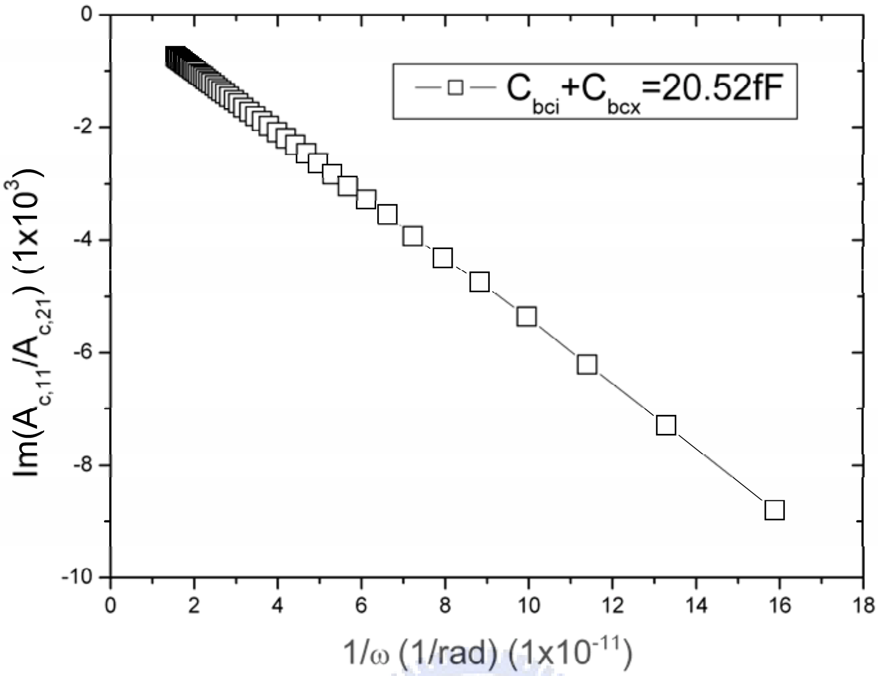

Fig.2-18 Plot of Im($A_{c,11}/A_{c,21}$) versus 1/ω. V_{BE}=0.83V, V_{CE}=3V, I_C=1.516mA, and I_B=9.136μA.

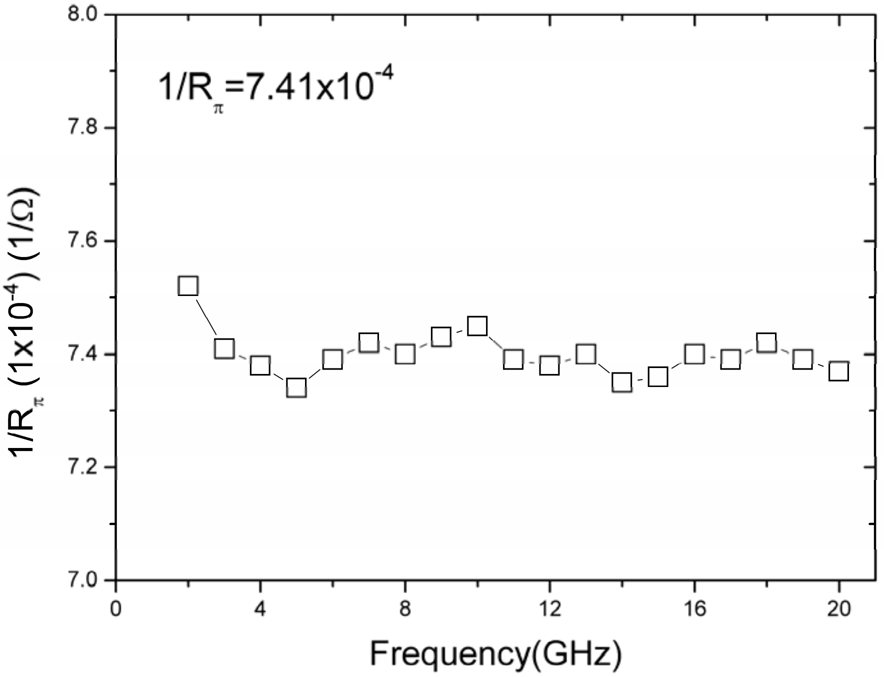

Fig.2-19 Frequency dependence of extracted 1/R_π for a SiGe HBT biased at V_{BE}=0.83V, V_{CE}=3V, I_C=1.516mA, and I_B=9.136μA.

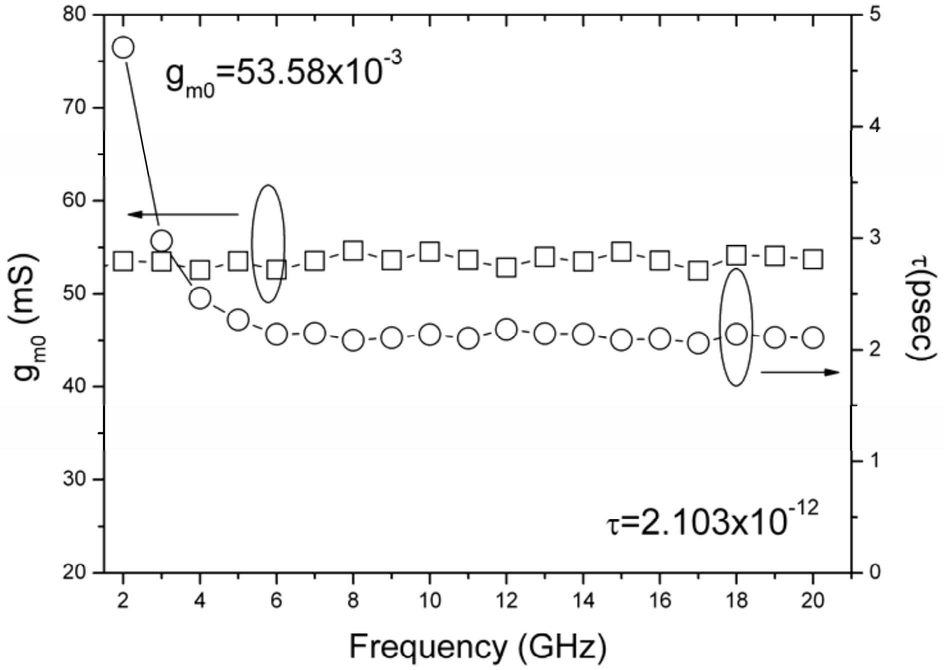

Fig.2-20 Frequency dependence of extracted g_{m0} and τ for a SiGe HBT biased at V_{BE}=0.83V, V_{CE}=3V, I_C=1.516mA, and I_B=9.136μA.

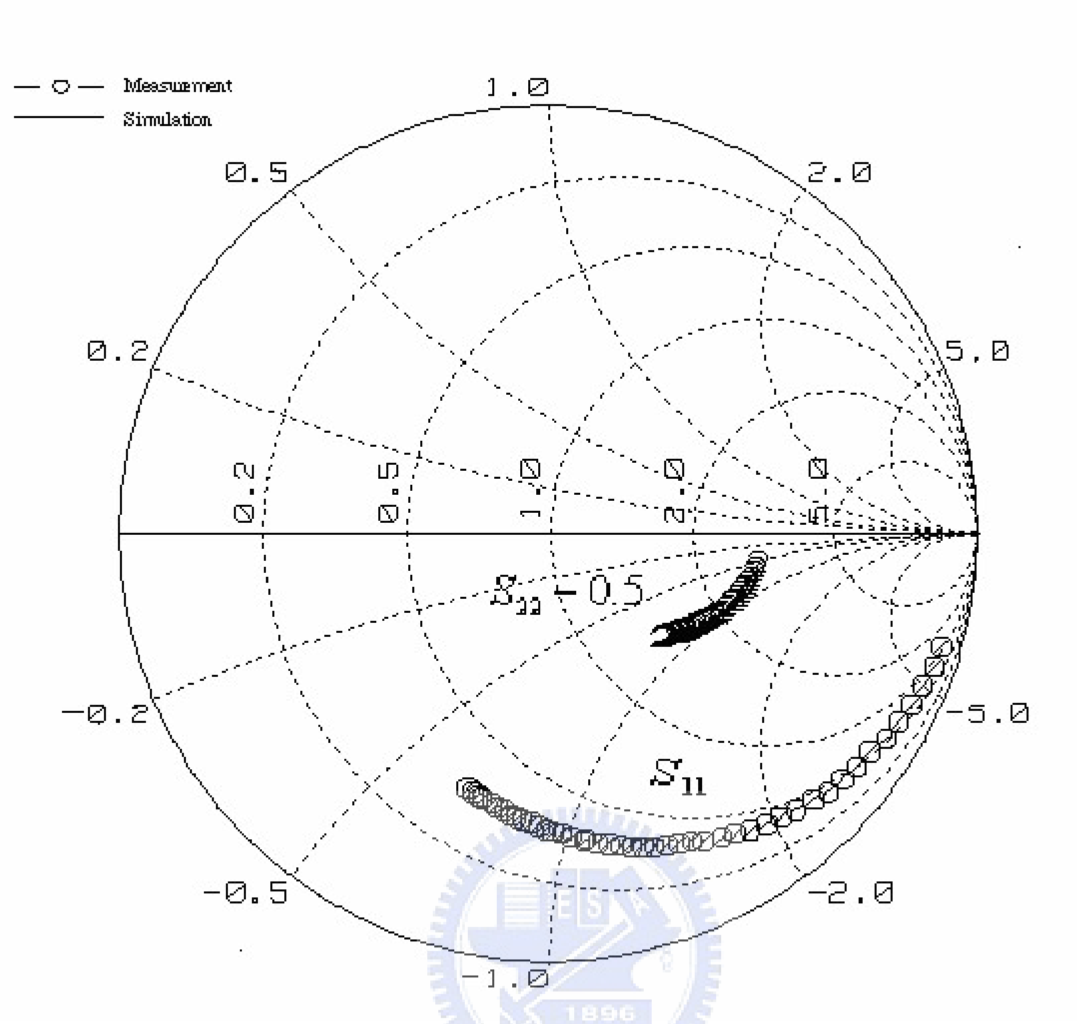

Fig.2-21 Measured and simulated S_{11} and S_{22} of the 4×0.24×32 μm^2 SiGe HBT in the frequency range of 1–20 GHz biased at V_{BE}=0.83V, V_{CE}=3V, I_B=9.136μA, and I_C=1.516mA.

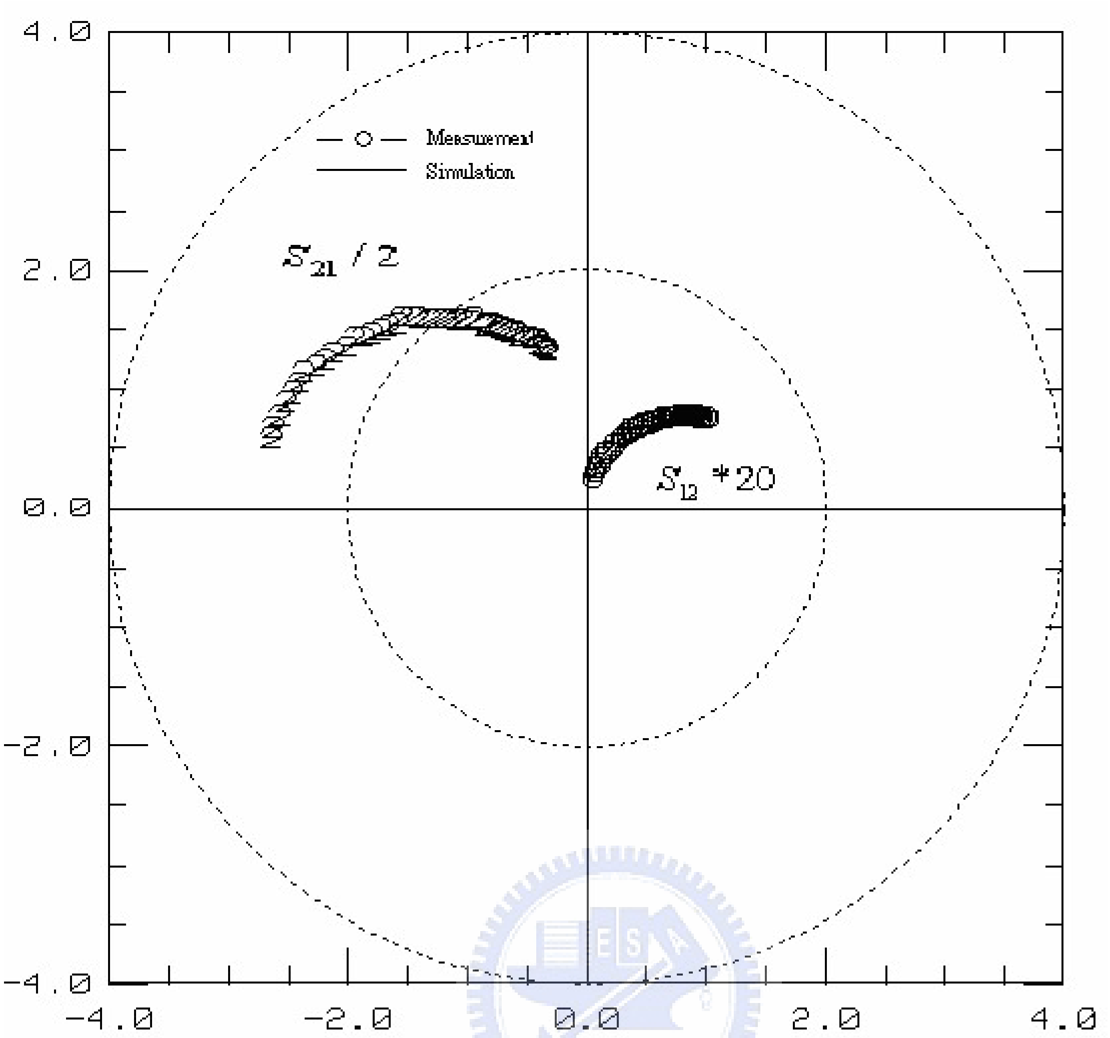

Fig.2-22 Measured and simulated S_{12} and S_{21} of the 4×0.24×32 μm^2 SiGe HBT in the frequency range of 1–20 GHz biased at V_{BE}=0.83V, V_{CE}=3V, I_B=9.136μA, and I_C=1.516mA.